tvst

Article

# Region of Interest Densitometry Analysis of Descemet Membrane Endothelial Keratoplasty Dehiscence on Anterior Segment Optical Coherence Tomography

**Albert Y. Cheung[1,2], Andrew Kalina[3,4], Alex Im[4], Andrew R. Davis[2], Medi Eslani[5], Raymond L. Hogge[1], and Elizabeth Yeu[1,2]**

[1] Virginia Eye Consultants/CEI Vision Partners, Norfolk, VA, USA
[2] Eastern Virginia Medical School, Department of Ophthalmology, Norfolk, VA, USA
[3] University of Kansas, Department of Ophthalmology, Kansas City, KS, USA
[4] Eastern Virginia Medical School, Norfolk, VA, USA
[5] Shiley Eye Institute, Viterbi Family Department of Ophthalmology, University of California San Diego, San Diego, CA, USA

**Correspondence:** Albert Y. Cheung, 241 Corporate Blvd, Norfolk, VA 23502, USA.
e-mail: acheung@cvphealth.com

**Received:** July 9, 2021
**Accepted:** September 7, 2021
**Published:** October 5, 2021

**Keywords:** densitometry; optical density; anterior segment optical coherence tomography; Descemet membrane endothelial keratoplasty; graft dehiscence

**Citation:** Cheung AY, Kalina A, Im A, Davis AR, Eslani M, Hogge RL, Yeu E. Region of interest densitometry analysis of descemet membrane endothelial keratoplasty dehiscence on anterior segment optical coherence tomography. Transl Vis Sci Technol. 2021;10(12):6, https://doi.org/10.1167/tvst.10.12.6

**Purpose:** To evaluate a region of interest (ROI) method of analyzing anterior segment optical coherence tomography (AS-OCT) corneal densitometry (CD) in the setting of Descemet membrane endothelial keratoplasty (DMEK) dehiscence.

**Methods:** Retrospective chart review of eyes that underwent (1) DMEK for Fuchs dystrophy (2) between 2018 to 2020 with (3) a partial DMEK dehiscence on AS-OCT, (4) involvement of only one side of the graft, (5) high-quality corneal AS-OCT scan, and (6) location of dehiscence within the central 5.5 mm of the cornea. Image analysis of the ROIs with ImageJ compared the total edematous area, mean stromal CD, and ratio of anterior-to-posterior (A/P) stromal CD for regions of DMEK dehiscence compared to the contralateral side with an attached DMEK graft. Control regions (with no dehiscence) and postdehiscence resolution images were also analyzed.

**Results:** Seventy sectors of the 21 images from 21 eyes with DMEK dehiscence were included. Compared to the contralateral side, regions of DMEK dehiscence had larger total areas ($P < 0.0001$), lower mean stromal CD ($P = 0.0003$), and higher A/P stromal CD ($P < 0.0001$). All control regions and postdehiscence resolution images did not show any significant differences compared to the contralateral sides.

**Conclusions:** This technique to analyze multiple ROIs on AS-OCT can be useful to evaluate CD of specific regions of corneal pathology. Lower mean stromal CD and higher A/P stromal CD may specify corneal edema.

**Translational Relevance:** Analyzing CD via multiple specific ROIs may be more suitable than measuring the CD of the full cornea and has broader applications extending to other corneal pathologies.

## Introduction

Corneal densitometry (CD) or optical density is an objective method for monitoring corneal transparency (backscattered light) in the setting of corneal refractive procedures and various corneal diseases.[1–6] Nearly all of the recent publications on CD use the Pentacam (Oculus Optikgeräte GmbH, Wetzlar, Germany), a rotating Scheimpflug camera. There are limitations with the Pentacam software in analyzing CD for specific areas of interest in the cornea. Compared to anterior segment optical coherence tomography (AS-OCT), it can be difficult to view let alone select a specific area for CD analysis if it is not confined to a specific annular zone or layer with the Pentacam software.

Endothelial keratoplasty procedures, such as Descemet's membrane endothelial keratoplasty (DMEK) and Descemet's stripping (automated) endothelial keratoplasty (DSAEK), have become

the preferred treatment for corneal endothelial disease and dysfunction (e.g., Fuchs dystrophy, pseudophakic bullous keratopathy) because they allow selective replacement of the diseased endothelium.[7] A true anatomic replacement of diseased Descemet's membrane and endothelium, DMEK appears to be superior to DSAEK,[8] but the surgical difficulty and unpredictability (especially associated with the learning curve) has limited its widespread adoption. Additionally, partial or complete graft detachment after surgery can be a relatively common complication of DMEK, ranging from 10% to 63%.[9–14]

In 2019, we presented a novel method on analyzing multiple region of interests (ROI) in the AS-OCT (Spectralis, Heidelberg, Germany) images of normal eyes, specifically studying the relationship between maximum epithelial reflectance and average stromal optical density (IOVS 2019;60:ARVO E-Abstract PB0136). Wertheimer et al.[15] recently published their method for CD analysis using the Carl Zeiss Cirrus HD-OCT 5000. They encompassed the central 6.4 mm of the cornea as a large ROI and compared separate images. We sought to expand on our previous work by comparing multiple smaller ROIs on the same image of corneal pathology. Partial DMEK graft dehiscence lends itself well to this analysis because there are particular areas of pathology and other areas of normal cornea (edematous areas and nonedematous areas, respectively) on the same image. In this way, there are also no concerns for comparing separate images with the need for corrective factors (i.e., for different image quality or background lighting).

# Methods

## Patient Selection and Data Collection

This study was conducted according to a protocol approved by the Eastern Virginia Medical School Institutional Review Board (Norfolk, VA, USA). The protocol and methods used also complied with the standards set forth by the Declaration of Helsinki. The study cohort consisted of a retrospective series of eyes that underwent DMEK for Fuchs dystrophy between 2018 to 2020. Inclusion criteria were (1) a documented area of partial DMEK dehiscence on AS-OCT, (2) involvement of only one side of the DMEK graft, (3) high-quality corneal AS-OCT scan (quality index $\geq$25 and $\leq$34), and (4) located within the central 5.5 mm of the cornea. Exclusion criteria comprised (1) presence of significant image artifact (e.g., peak air density, significant bullae causing reverse shadowing, see Fig. 1), (2) significant corneal scarring, (3) poor OCT quality precluding image analysis for any other reason, and (4) presence of DMEK dehiscence on both sides of the graft (precluding comparison of the dehisced section with a contralateral section overlying attached graft). All OCTs were performed on a Heidelberg Spectralis imaging platform (Heidelberg Engineering, Carlsbad, CA) with the Anterior Segment Module to obtain high-resolution OCT imaging of the cornea. High-resolution multi-line scans were obtained. Because the Heidelberg Spectralis uses spectral-domain OCT, we neglected the peripheral cornea outside of 5.5 mm because of the decreased signal strength (less light reflected back) resulting in more difficulty in interpreting peripheral data. This

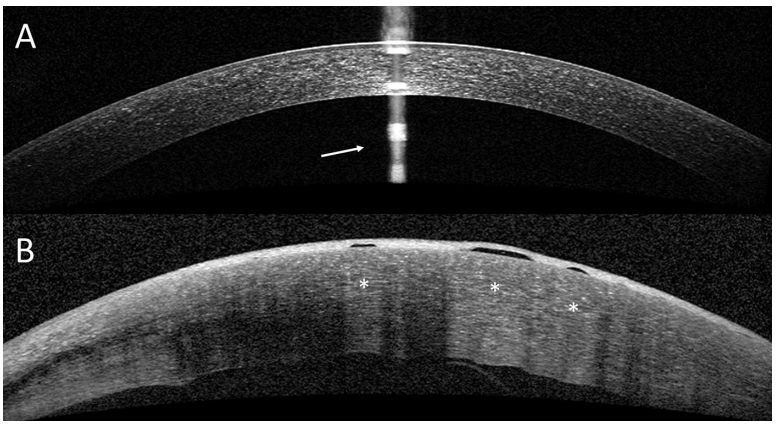


**Figure 1.** Anterior segment optical coherence tomography images demonstrating examples of image artifacts such as peak air density (A, *arrow*) and significant bullae causing reverse shadowing (B, *asterisk*). The reverse shadowing gives an area of hyperintensity posterior to the epithelial bullae.

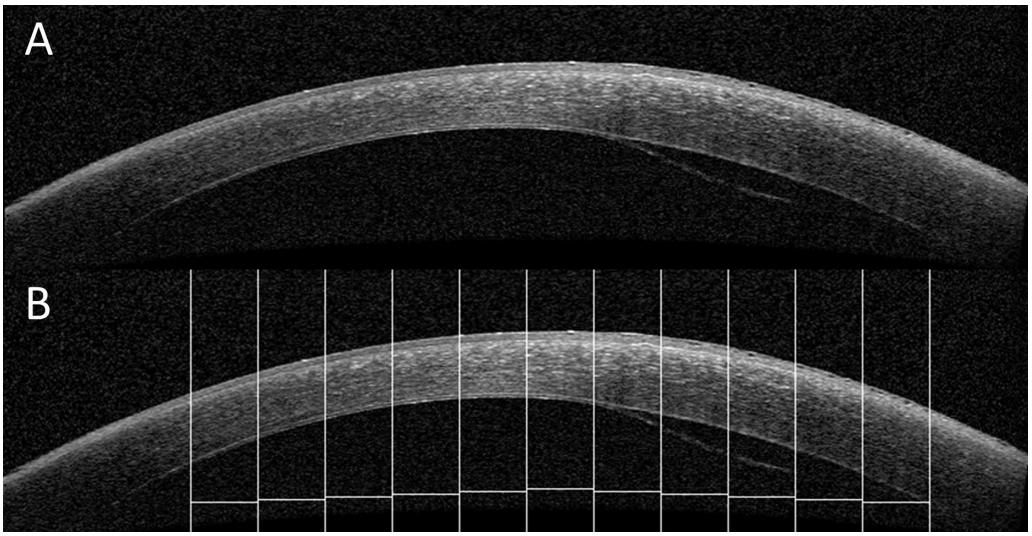


**Figure 2.** Example of image analysis. (A) The image of partial DMEK detachment. (B) A macro for region of interest is run, which divides the central 5.5 mm into 11 sectors (500 µm each).

is in contrast to swept-source OCT, which is much better at imaging outside of this central area because it uses a longer wavelength. Demographic, clinical, and imaging data were collected on all patients including age, gender, AS-OCT images that met the inclusion criteria, and AS-OCT images of the same eyes after dehiscence resolution.

## OCT Imaging and CD Measurements

Data were exported from the OCT acquisition software as gray-scale TIFF images. The highest-quality image within the quality range from each eye/dehiscence was selected. The images were analyzed using ImageJ (National Institutes of Health; http://rsbweb.nih.gov/ij/). The corneal apex was identified by drawing a horizontal line tangent to the cornea. With the coordinates of the corneal apex, an ImageJ macro was created to measure the central 5.5 mm of the cornea and divide this area into 11 sectors (500 µm each, see Fig. 2B). The ImageJ ROI manager is a tool to work with and analyze multiple selections (e.g., points, lines, shapes) from either the same image or different images. Using the ROI manager tool, the full stromal area (area between epithelium/Bowman's and Descemet) of each sector was selected (Fig. 3A), and the average gray value within each selection was measured (range between 0 corresponding to pure black and 255 corresponding to pure white). An average value (or mean stromal CD) of the ROI was calculated as the sum of all the gray value pixels in a selection divided by the number of pixels. This is a similar protocol to the one previously described for evaluating optical density in retinal OCT images using Heidelberg Spectralis.[16–18] Previous studies measuring optical density with retinal OCTs expressed ROI values as an optical density ratio to account for overlying media opacities (i.e., lens, vitreous).[16–18] This was not necessary for corneal AS-OCTs because the overlying air would not be a confounding factor.

Other measured values were total stromal area of each sector (stroma in the sector above the dehiscence) and the ratio of anterior-to-posterior (A/P) stromal CD. A/P stromal CD measurements were taken by dividing each sector into anterior and posterior halves. Each half was made into a ROI, and the mean stromal CD was measured (Fig. 3B). Briefly, each stromal sector was divided manually by determining the x- and y-axes (displayed on the ImageJ control panel while hovering over a point) for the epithelium/Bowman's and Descemet layer borders. The middle plane of each sector was calculated from these x- and y-axes of the borders and used to create the anterior and posterior halves of each sector using the polygon shape selection tool. There was a minimum of six points to outline each sector half.

We previously presented AS-OCT data in normal eyes demonstrating that the mean stromal CD decreased with respect to lateral position in a linear or quadratic manner (ie. sectors further from the corneal apex had lower mean stromal CD, IOVS 2019;60:ARVO E-Abstract PB0136). There was also a parabolic relationship between mean stromal CD and position (ie. corresponding contralateral sectors had similar mean stromal CD). Given this mirrored, parabolic relationship in normal eyes, measurements for regions of DMEK dehiscence were compared to the contralateral side with the attached DMEK graft (control regions). The apex sector (position 1,

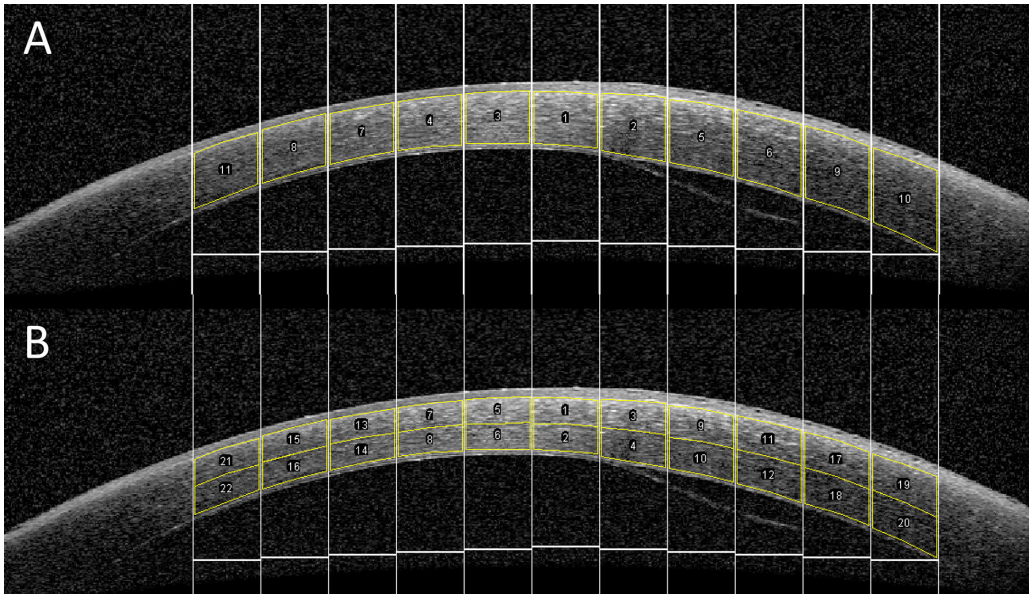


**Figure 3.** Example of image analysis. (A) The region of interest (ROI) tool is used to select the stroma of each sector. (B) Each stromal sector is divided into anterior and posterior halves and selected with the ROI tool.

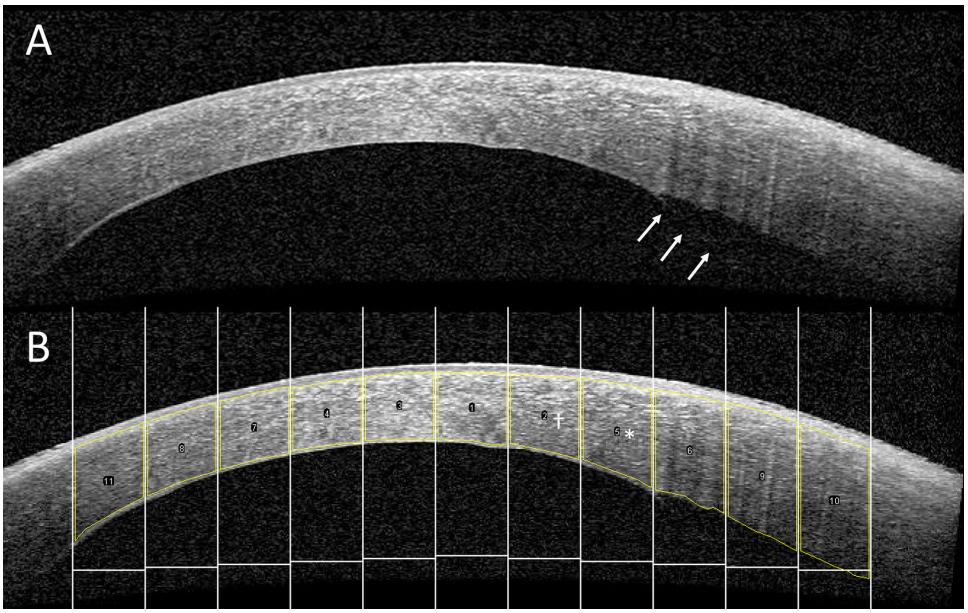


**Figure 4.** Example of image analysis. (A) Another image of partial DMEK detachment (*arrows*). (B) Adjacent sector (*asterisk*) to the DMEK dehiscence and sectors 2 away (*dagger*) from the dehiscence are shown in this image.

see Fig. 3A) was not included as there was no corresponding contralateral sector for comparison. Additionally, AS-OCT scans of the same areas of the DMEK dehiscence were analyzed similarly after resolution of the dehiscence. For additional comparison, sectors that were directly adjacent and two sectors away from the sectors overlying the dehiscence were compared to the contralateral side without dehiscence (see Fig. 4).

## Statistical Analysis

Statistical analysis was performed using SPSS software (version 21.0; IBM Corp., Armonk, NY, USA). The normality of the data was tested using the D'Agostino and Pearson normality tests. Next, a two-tailed *t*-test and Mann Whitney test were then used to compare the data, with $P < 0.05$ considered statistically significant.

## Results

During the retrospective period, there were 22 DMEK eyes that had a documented area of partial DMEK dehiscence on AS-OCT. One was excluded based on exclusion criteria because there was a dehiscence of the DMEK graft on both sides peripherally. After the available images were reviewed, a total of 70 sectors from 21 images of 21 eyes (20 patients; 12 male, 8 female; mean age 65.78 ± 8.18 years) with DMEK dehiscence were included. All eyes had Fuchs and underwent uncomplicated DMEK (n = 10) or combined DMEK with cataract extraction (n = 11).

Of the 70 sectors overlying a detached DMEK graft, the mean area of these sectors was 0.35 ± 0.06; the mean area of contralateral sectors overlying an attached DMEK graft was 0.28 ± 0.06. The mean stromal area overlying the regions of DMEK dehiscence was significantly larger ($P < 0.0001$). The mean stromal CD (83.53 ± 22.26) of DMEK dehiscence areas was significantly lower than the contralateral side (98.28 ± 25.09, $P = 0.0003$). There was a significantly higher A/P stromal CD (mean 1.87 ± 0.54) for DMEK dehiscence areas compared to the contralateral side (mean 1.49 ± 0.26, $P < 0.0001$).

The sector adjacent to the dehisced DMEK (n = 18) was studied and had a larger overlying stromal area (0.29 ± 0.05) compared to the contralateral side (0.26 ± 0.05, $P = 0.0559$). There was also a lower mean stromal CD for adjacent sectors (108.80 ± 20.20) compared to the contralateral side (116.30 ± 25.48, $P = 0.3364$). Although these both were not statistically significant, there was a significant difference between adjacent sectors (1.51 ± 0.19) compared to the contralateral side (1.33 ± 0.14, $P = 0.0026$) for A/P stromal CD values. There were 11 images that had sectors two away from the dehiscence area that were available for comparison to the contralateral side. These all had similar values compared to the contralateral side, and none of the outcome measures were statistically significant. Additionally, control areas (unaffected sectors on the side of the dehiscence) were compared to contralateral side. There were no significant differences for this comparison. The Table displays the values and comparisons for all these groups.

**Table.** AS-OCT Region of Interest Analysis Data

| Variable | DMEK Dehiscence [Range] | No Dehiscence (Contralateral Side) [Range] | *P* Value |
|---|---|---|---|
| N (image sectors analyzed) | 70 | 70 | |
| Mean total area (mm$^2$) | 0.35 ± 0.07 [0.17–0.51] | 0.28 ± 0.06 [0.13–0.39] | <0.0001 |
| Mean stromal CD | 83.53 ± 22.26 [37.01–124.7] | 98.28 ± 25.09 [36.73–148.6] | 0.0003 |
| A:P stromal CD | 1.87 ± 0.54 [1.16–3.86] | 1.49 ± 0.26 [1.11–2.53] | <0.0001 |
| | Sector adjacent to the dehisced DMEK | Contralateral side | |
| N (image sectors analyzed)* | 18 | 18 | |
| Mean total area (mm$^2$) | 0.29 ± 0.05 [0.15–0.36] | 0.26 ± 0.05 [0.13–0.32] | 0.06 |
| Mean stromal CD | 108.80 ± 20.20 [64.80–138.50] | 116.30 ± 25.48 [79.43–166.40] | 0.34 |
| A:P stromal CD | 1.51 ± 0.19 [1.16–1.91] | 1.33 ± 0.14 [1.11–1.59] | 0.0026 |
| | Sector 2 away from the dehisced DMEK | Contralateral side | |
| N (image sectors analyzed)* | 11 | 11 | |
| Mean total area (mm$^2$) | 0.26 ± 0.04 [0.18–0.34] | 0.25 ± 0.04 [0.17–0.32] | 0.50 |
| Mean stromal CD | 119.00 ± 24.50 [78.55–152.20] | 124.30 ± 27.52 [86.43–182.70] | 0.63 |
| A:P stromal CD | 1.38 ± 0.14 [1.10–1.59] | 1.27 ± 0.14 [1.01–1.49] | 0.10 |
| | Control/attached DMEK | Contralateral side | |
| N (image sectors analyzed) | 6 | 6 | |
| Mean total area (mm$^2$) | 0.24 ± 0.02 [0.20–0.26] | 0.23 ± 0.02 [0.20–0.25] | 0.46 |
| Mean stromal CD | 126.20 ± 27.72 [90.92–156.00] | 124.50 ± 20.59 [93.03–147.60] | 0.90 |
| A:P stromal CD | 1.29 ± 0.13 [1.15–1.52] | 1.26 ± 0.09 [1.13–1.36] | 0.94 |
| | Postresolution | Contralateral side | |
| N (image sectors analyzed) | 69 | 69 | |
| Mean total area (mm$^2$) | 0.23 ± 0.03 [0.16–0.30] | 0.24 ± 0.04 [0.16–0.32] | 0.31 |
| Mean stromal CD | 89.05 ± 26.14 [35.03–139.50] | 88.74 ± 29.49 [26.75–150.50] | 0.95 |
| A/P stromal CD | 1.53 ± 0.35 [1.09–2.88] | 1.51 ± 0.33 [1.09–3.01] | 0.95 |

N, number.

*Differences in sample sizes were dependent on the dehiscence size because there needed to be a comparison on the contralateral side. The sector two away from a large dehiscence might be on the contralateral side and thus would not have a "normal" contralateral comparison.

Postdehiscence resolution images that corresponded with the areas of prior DMEK dehiscence were compared to the contralateral side. There were no significant differences for mean total area, mean stromal CD, and A/P stromal CD.

## Discussion

CD is a measure of the corneal light backscatter expressed in gray scale units.[19] CD has previously been studied in DMEK, but these studies were all done with Scheimpflug imaging (i.e., Oculus Pentacam; Oculus, Wetzlar, Germany).[2,20–27] Limitations in the Pentacam software do not allow for selection of specific regions of interest for CD measurement. Rather, studied areas are typically confined to four annular zones (0–2 mm, 2–6 mm, 6–10 mm, and 10–12 mm) and four corneal layers (anterior, posterior, central, and total). In this study, ImageJ analysis of AS-OCT images allowed for specific selection of involved sectors. Here, the contour of the involved stromal area was selected, and a CD measurement was generated. The ROI feature allows for outlining of a custom polygon shape (see Fig. 4B), not just a simple square or rectangle. This was applied to the irregular shapes of the edematous corneas in this study, as well as the anterior and posterior aspects of a specific sector. This technique has further future applications because any area of the imaged cornea can be selected as an ROI for comparison (i.e., focal area of edema or scarring, specific corneal deposits, neoplasms, vessels, etc.).

We compared extremely edematous states (dehisced Descemet membrane) with relative nonedematous states (attached Descemet's membrane) and found stromal CD was significantly decreased in the areas of dehisced Descemet membrane. This is interesting because edematous states typically have less corneal clarity and more backscatter. Previous studies with Scheimpflug imaging demonstrated increased CD in edematous states following DMEK surgery which decreased as the eyes were followed longitudinally.[21,23,25–27] To explain the decreased CD in our dehisced DMEK areas, the darker images (decreased CD) on AS-OCT may represent aqueous fluid percolating through the stroma and creating small pockets of fluid (because fluid is seen as dark on AS-OCT, e.g., epithelial bullae). The edematous lamellar separations lead to decreased CD. Interestingly, certain images demonstrated a hyperintensity of epithelium/Bowman's and even anterior stroma (see Fig. 4 and to a lesser extent Fig. 2), possibly related to microcystic edema, epithelial thickening, and adjacent back light scattering or edema-related interface changes between the fluid and collagen fibrils. There may be a component of resultant signal attenuation that contributed to the decrease CD. However, a review of the images noted that this hyperintensity was only variably present (see Fig. 5), so signal attenuation would not fully explain the decreased CD. It also does not appear that this decreased CD is an artifact of less light reflecting back from Descemet's membrane as even adjacent areas with attached Descemet's membrane (and edematous stroma) also demonstrated decreased stromal CD. Although these adjacent areas did not show a significant difference from contralateral control areas, the sample size was quite small. Further studies are needed to investigate these different changes in corneal transparency based on the imaging modality and corneal pathology.

Comparing the anterior and posterior stromal CD (i.e., A/P value) of a sector demonstrated another way to compare edematous corneal areas to nonedematous ones. Increased A/P stromal CD values in areas of

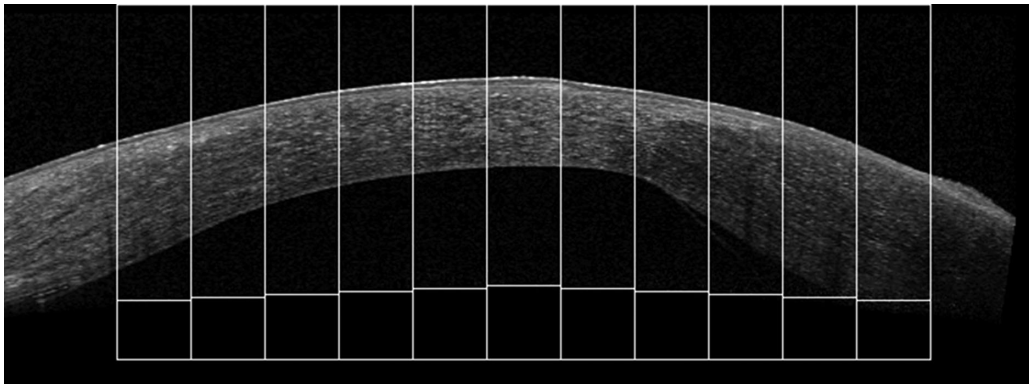

**Figure 5.** Example of DMEK dehiscence without hyperintensity of epithelium/Bowman and anterior stroma. Obvious bullae or microcystic edema in epithelium are not present here either.

dehisced DMEK grafts showed that the edema affected the posterior stroma to a greater extent. This would be expected because the posterior stroma is exposed directly to aqueous without any intervening Descemet tissue. This may be an internal measure to detect edema when no contralateral control area is available for comparison. Even in the excluded DMEK eye with dehiscence on both sides, the A/P stromal CD values of both areas were elevated (1.74 and 1.76). Further studies are needed to determine normal A/P stromal CD values and how it varies by position.

Comparison of control sectors (sectors over attached DMEK and three or more sectors away from the DMEK dehiscence) with the contralateral side confirmed our previous findings of a parabolic relationship between mean stromal CD and position (i.e., corresponding contralateral sectors had similar mean stromal CD). Additionally, postdehiscence resolution images showed no difference between the two sides. This parabolic relationship may be attributed to less light being directly reflected back to the OCT device because the light is not hitting directly at the normal to the surface in the peripheral cornea (i.e., the further one moves laterally from the central cornea).

Compared to Pentacam full corneal cross-sectional images, AS-OCT images with the Heidelberg Spectralis have increased image resolution despite poorer field of view. Examining various corneal pathologies is more easily facilitated. This also allows for ROI selection of specific layers or areas for CD analysis. Despite this, it should be noted that on some images in the current study, Bowman's layer could not always be distinctly delineated. However, any inclusion or exclusion of this on image analysis would not have significantly altered the mean stromal CD values that were measured.

Although this technique of evaluating DMEK dehiscence is likely unnecessary to diagnose and follow most graft dehiscences clinically, it may be indicated to confirm areas of corneal edema with shallow detachments or demonstrate improvement after a rebubble with slow progress. Rather, this study was designed to propose an expanded technique for ROI CD analysis. Here, we not only compared multiple ROIs within the same image laterally (areas of dehiscence versus areas of graft attachment), but we also evaluated the anterior and posterior stroma with ROI analysis. The latter analysis (ratios of CD) may be valuable in characterizing how different areas of the cornea (anterior vs. posterior) may be affected with a particular pathology and help to study other edematous states. Our analysis differed from Wertheimer et al in that we did not look at a significant intensity threshold for corneal optical density evaluation but rather the mean stromal CD of a ROI.[15] Additionally, there can be concerns of comparing separate AS-OCT images if not accounting for the background lighting or image quality without a corrective factor. Because our images made comparisons on the same image, this was not a concern.

This study was not without other limitations. Given its retrospective nature, there were limited images to select from, with only certain images meeting the quality inclusion criteria. There also is inter-scan variability in regards to the quality and lighting (brightness/contrast), which may affect the grayscale baseline of an image. This prevented comparison of pathology on separate scans without a corrective factor. However, scans with partial DMEK dehiscence (having areas of both edema and normalized, compact cornea in the same image) were studied for this reason since there was no need to account for the variability in image quality and lighting. In the future, A/P stromal CD may prove to be useful in comparison of separate AS-OCT images because it provides an inherent correction factor since it is a ratio.

We describe a method to analyze CD for multiple ROIs on AS-OCT images. This may be useful to evaluate the CD of any specific region of corneal pathology. This was the first study applying ROI AS-OCT analysis for DMEK cases. For cases of DMEK dehiscence, we found these sectors had greater total area, lower mean stromal CD, and a higher A/P stromal CD compared to control unaffected areas. These later two image characteristics may help to identify corneal edema.

## Acknowledgments

Disclosure: **A.Y. Cheung,** Alcon (C), LayerBio (C); **A. Kalina,** None; **A. Im,** None; **A.R. Davis,** None; **M. Eslani,** None; **R.L. Hogge,** None; **E. Yeu,** Alcon (C), Allergan (C), Avedro (C), Bausch & Lomb/Valeant (C), Beaver Visitec (C), Bruder (C), EyePoint Pharmaceuticals (C), Glaukos (C), iOptics (C), Guidepoint (C), J & J Vision (C), LENSAR (C), Kala Pharmaceuticals (C), Novartis (C), Ocular Science (C), Ocular Therapeutix (C), Ocusoft (C), Omeros (C), Oyster Point Pharma (C), Science Based Health (C), Shire (C), Sight Sciences (C), SightLife Surgical (C), Sun (C), Tissue-Tech (C), TopCon (C), TearLab Corporation (C), TearScience (C), and Zeiss (C)

## References

1. Wang J, Thomas J, Cox I. Corneal light backscatter measured by optical coherence tomography after LASIK. *J Refract Surg*. 2006;22:604–610.

2. Alnawaiseh M, Zumhagen L, Wirths G, Eveslage M, Eter N, Rosentreter A. Corneal densitometry, central corneal thickness, and corneal central-to-peripheral thickness ratio in patients with Fuchs endothelial dystrophy. *Cornea.* 2016;35:358–362.
3. Greenstein SA, Fry KL, Bhatt J, Hersh PS. Natural history of corneal haze after collagen crosslinking for keratoconus and corneal ectasia: Scheimpflug and biomicroscopic analysis. *J Cataract Refract Surg.* 2010;36:2105–2114.
4. Enders P, Holtick U, Schaub F, et al. Corneal densitometry for quantification of corneal deposits in monoclonal gammopathies. *Cornea.* 2017;36:470–475.
5. Elflein HM, Hofherr T, Berisha-Ramadani F, et al. Measuring corneal clouding in patients suffering from mucopolysaccharidosis with the Pentacam densitometry programme. *Br J Ophthalmol.* 2013;97:829–833.
6. Kamiya K, Kobashi H, Takahashi M, Shoji N, Shimizu K. Effect of scattering and aberrations on visual acuity for band keratopathy. *Optom Vis Sci.* 2017;94:1009–1014.
7. Lee WB, Jacobs DS, Musch DC, Kaufman SC, Reinhart WJ, Shtein RM. Descemet's stripping endothelial keratoplasty: safety and outcomes: a report by the American Academy of Ophthalmology. *Ophthalmology.* 2009;116:1818–1830.
8. Deng SX, Lee WB, Hammersmith KM, et al. Descemet membrane endothelial keratoplasty: safety and outcomes: a report by the American Academy of Ophthalmology. *Ophthalmology.* 2018;125:295–310.
9. Deng SX, Sanchez PJ, Chen L. Clinical outcomes of Descemet membrane endothelial keratoplasty using eye bank-prepared tissues. *Am J Ophthalmol.* 2015;159:590–596.
10. Ham L, Dapena I, Liarakos VS, et al. Midterm results of Descemet membrane endothelial keratoplasty: 4 to 7 years clinical outcome. *Am J Ophthalmol.* 2016;171:113–121.
11. Price MO, Giebel AW, Fairchild KM, Price FW, Jr. Descemet's membrane endothelial keratoplasty: prospective multicenter study of visual and refractive outcomes and endothelial survival. *Ophthalmology.* 2009;116:2361–2368.
12. Rodriguez-Calvo-de-Mora M, Quilendrino R, Ham L, et al. Clinical outcome of 500 consecutive cases undergoing Descemet's membrane endothelial keratoplasty. *Ophthalmology.* 2015;122:464–470.
13. Woo JH, Ang M, Htoon HM, Tan D. Descemet membrane endothelial keratoplasty versus Descemet stripping automated endothelial keratoplasty and penetrating keratoplasty. *Am J Ophthalmol.* 2019;207:288–303.
14. Dirisamer M, van Dijk K, Dapena I, et al. Prevention and management of graft detachment in Descemet membrane endothelial keratoplasty. *Arch Ophthalmol.* 2012;130:280–291.
15. Wertheimer CM, Elhardt C, Wartak A, et al. Corneal optical density in Fuchs endothelial dystrophy determined by anterior segment optical coherence tomography. *Eur J Ophthalmol.* 2021;31:1771–1778.
16. Ahlers C, Golbaz I, Einwallner E, et al. Identification of optical density ratios in subretinal fluid as a clinically relevant biomarker in exudative macular disease. *Invest Ophthalmol Vis Sci.* 2009;50:3417–3424.
17. Neudorfer M, Weinberg A, Loewenstein A, Barak A. Differential optical density of subretinal spaces. *Invest Ophthalmol Vis Sci.* 2012;53:3104–3110.
18. Kashani AH, Cheung AY, Robinson J, Williams GA. Longitudinal optical density analysis of subretinal fluid after surgical repair of rhegmatogenous retinal detachment. *Retina.* 2015;35:149–156.
19. Lopes B, Ramos I, Ambrosio R, Jr. Corneal densitometry in keratoconus. *Cornea.* 2014;33:1282–1286.
20. van Dijk K, Rodriguez-Calvo-de-Mora M, van Esch H, et al. Two-Year Refractive Outcomes After Descemet Membrane Endothelial Keratoplasty. *Cornea.* 2016;35:1548–1555.
21. Schaub F, Enders P, Bluhm C, Bachmann BO, Cursiefen C, Heindl LM. Two-year course of corneal densitometry after Descemet membrane endothelial keratoplasty. *Am J Ophthalmol.* 2017;175:60–67.
22. Schaub F, Gerber F, Adler W, et al. Corneal densitometry as a predictive diagnostic tool for visual acuity results after Descemet membrane endothelial keratoplasty. *Am J Ophthalmol.* 2019;198:124–129.
23. Agha B, Dawson DG, Kohnen T, Schmack I. Corneal densitometry after secondary Descemet membrane endothelial keratoplasty. *Cornea.* 2019;38:1083–1092.
24. Augustin VA, Weller JM, Kruse FE, Tourtas T. Can we predict the refractive outcome after triple Descemet membrane endothelial keratoplasty? *Eur J Ophthalmol.* 2019;29:165–170.

25. Droutsas K, Lazaridis A, Giallouros E, Kymionis G, Chatzistefanou K, Sekundo W. Scheimpflug densitometry after DMEK versus DSAEK-two-year outcomes. *Cornea.* 2018;37:455–461.
26. Lazaridis A, Fydanaki O, Giallouros E, et al. Recovery of corneal clarity after DMEK followed by rebubbling versus uneventful DMEK. *Cornea.* 2018;37:840–847.
27. Satue M, Idoipe M, Gavin A, et al. Early changes in visual quality and corneal structure after DMEK: does DMEK approach optical quality of a healthy cornea? *J Ophthalmol.* 2018;2018:2012560.